Available online at www.sciencedirect.com
ScienceDirect
Bioorganic & Medicinal Chemistry 16 (2008) 400–404
Bioorganic & Medicinal Chemistry

Design of a pyrene-containing fluorescence probe for labeling of RNA poly(A) tracts

Kazuo Tanaka[a,b] and Akimitsu Okamoto[a,*]

[a]*Frontier Research System, RIKEN (The Institute of Physical and Chemical Research), Wako, Saitama 351-0198, Japan*
[b]*Department of Polymer Chemistry, Faculty of Engineering, Kyoto University, Kyoto 615-8510, Japan*

Received 21 August 2007; revised 12 September 2007; accepted 13 September 2007
Available online 18 September 2007

Abstract—A labeling probe containing a pyrenecarboxamide-tethered modified DNA base, ^{Py}U, has been developed for fluorometric detection of RNA poly(A) tracts, in which the fluorescence emission intensity was controlled by the microstructural change around ^{Py}U caused by binding with the target RNA.

1. Introduction

Recent advances in fluorescence microscopy, imaging, and probe technology have enabled the rapid monitoring of the spatial and temporal distribution of RNA. A fluorescent in situ hybridization method using a fluorescence-labeled DNA, such as a molecular beacon technique by a doubly labeled DNA, has been developed so far for the marking of a sequence of poly(A), which most eukaryotic mRNAs have at the 3′-termini.[1,2] The design of fluorescence-labeled DNA has become a central feature of new chemistry-based biotechnology because of the great potential of modified oligonucleotides as diagnostic tools in molecular biology.

Modified oligonucleotides containing pyrene derivatives have been widely used for DNA and RNA quantification, single nucleotide polymorphism (SNP) typing, hybridization, and structural alteration.[3] The fluorescence of pyrene-1-carboxaldehyde is known to show a strong dependence on the solvent polarity,[4] so that the fluorescence of pyrene-1-carboxaldehyde is strong in methanol, but negligible in nonpolar solvents.[5] Using this unique characteristic, we developed a pyrenecarboxamide-tethered modified DNA base, ^{Py}U (Fig. 1), and applied it to SNP discrimination in DNA.[6] Fluorescence probes containing the ^{Py}U base selectively emit fluorescence only when the complementary base is A. In this case, the chromophore of ^{Py}U is extruded to the outside of the duplex because of Watson–Crick base pair formation, and exposed to a highly polar aqueous phase. In contrast, the duplex containing a ^{Py}U/N (N = G, C, and T) mismatched base pair shows a structure in which the glycosyl bond of uridine is rotated to the syn conformation. In this conformation, the chromophore is located at a hydrophobic site of the duplex. The control of base-specific fluorescence emission is based on the polarity change in the microenvironment where the chromophore locates dependent on the ^{Py}U/A base pair formation.

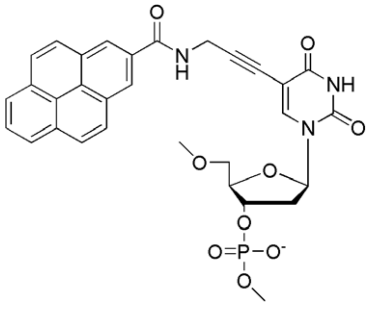

Figure 1. Chemical structure of ^{Py}U.

In this paper, we report a ^{Py}U-containing fluorescence probe for the labeling of poly(A) tracts in RNA. The fluorescence of the ^{Py}U-containing probe that we designed was quenched in the absence of poly(A) tracts, whereas the conformation of the probe changed in the presence of an RNA poly(A) tract and a much higher

Keywords: Fluorescence; DNA probes; Pyrene; RNA detection.
* Corresponding author. Tel.: +81 48 467 9238; fax: +81 48 467 9205; e-mail: aki-okamoto@riken.jp

0968-0896/$ - see front matter © 2007 Elsevier Ltd. All rights reserved.
doi:10.1016/j.bmc.2007.09.024

fluorescence intensity was observed. The conformation change upon hybridization with poly(A) resulted in a change in fluorescent intensity. Standard molecular beacon probes should include both of the fluorophores and the quenchers, and thus these modifications are troublesome. Our strategy would be advantageous for evolving fluorescence probes.

2. Results and discussion

We prepared a ^{Py}U-containing DNA, 5′-d(CGCAA T^{Py}UTAACGC)-3′ (**ODN**(^{Py}**U**)), and hybridized it with complementary DNA (**cDNA**) and RNA (**cRNA**). The results of fluorescence and absorption measurements are summarized in Figure 2 and Table 1. The fluorescence spectrum of **ODN**(^{Py}**U**)**/cDNA** showed a strong fluorescence at 440 nm after 350 nm excitation (Φ_F = 0.203). In contrast, the fluorescence of a DNA–RNA duplex, **ODN**(^{Py}**U**)**/cRNA**, was much weaker (Φ_F = 0.055). The wavelength of the absorption maximum, λ_{max}, of **ODN** (^{Py}**U**)**/cDNA** was 340 nm, which was close to the λ_{max} reported for the ^{Py}U nucleoside,[6] whereas the λ_{max} of **ODN**(^{Py}**U**)**/cRNA** and **ODN**(^{Py}**U**) itself were observed at 350 nm, suggesting that the chromophore was located on the inside of a higher-ordered structure (i.e., lower polarity microenvironment). In other words, lower stability of a ^{Py}U/A base pair in a DNA–RNA duplex resulted in a red shift in absorption and lower intensity of fluorescence emission, which is different from the photophysical behavior observed for a DNA–DNA duplex. Actually, the thermal stability of **ODN**(^{Py}**U**)**/cRNA** was low. To investigate the duplex stability, the melting temperature (T_m) of 2.5 μM ^{Py}U-containing duplexes was measured in sodium phosphate buffer (pH 7.0) and 100 mM sodium chloride (Table 1). Compared with native duplexes, the incorporation of ^{Py}U caused a decrease in T_m values. In particular, **ODN** (^{Py}**U**)**/cRNA** was significantly destabilized by the use of ^{Py}U-containing DNA. The low T_m value of

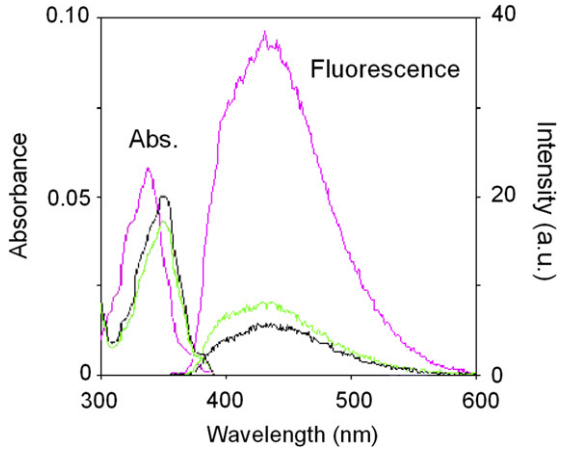

Figure 2. Spectral changes of 2.5 μM **ODN**(^{Py}**U**) (black line) hybridized with 2.5 μM **cDNA** (magenta line) or **cRNA** (green line) (50 mM sodium phosphate, 100 mM sodium chloride, pH 7.0, 25 °C). Excitation wavelength was 350 nm.

Table 1. Melting temperatures (T_m) and photophysical properties of ^{Py}U-containing DNA[a]

Sequences[b]	T_m (°C)	λ_{max} (nm)	ε_{max}[c]	Φ_F[d]
ODN(^{Py}**U**)		350	19,600	0.034
ODN(^{Py}**U**)**/cDNA**	50.7	340	23,200	0.203
ODN(^{Py}**U**)**/cRNA**	28.6	350	17,500	0.055
ODN(T)/cDNA	57.3			
ODN(T)/cRNA	47.4			

[a] The duplexes (2.5 μM) were measured in 50 mM sodium phosphate and 100 mM sodium chloride (pH 7.0) at 25 °C.
[b] **ODN(N)** = 5′-d(CGCAATNTAACGC)-3′ (N = ^{Py}U or T), **cDNA** = 5′-d(GCGTTAAATTGCG)-3′, **cRNA** = 5′-r(GCGTTAAATTCG C)-3′.
[c] ε_{max} is the molar extinction coefficient given at the peak of the absorption spectra.
[d] The calculation of fluorescence quantum yields (Φ_F) is described in experimental sections.

ODN (^{Py}**U**)**/cRNA** strongly suggests lower stability of the base pair between ^{Py}U and A in RNA.

Based on the experimental results described above, we designed a ^{Py}U-containing probe, **pODN**, for the labeling of an RNA poly(A) sequence (Fig. 3a). This probe usually has a hairpin conformation with a 7-base stem. A ^{Py}U/C mismatched base pair was incorporated in the stem region. The mismatched base pair would suppress the ^{Py}U fluorescence efficiently, because the chro-

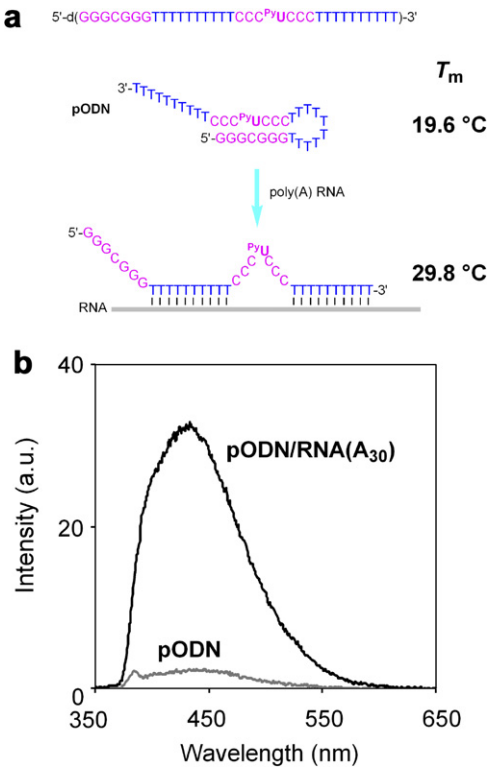

Figure 3. Newly designed ^{Py}U probe for RNA detection. (a) Sequence and schematic illustration of **pODN** for target detection. When **pODN** binds to the target, the intramolecular stem structure dissolves, and ^{Py}U is isolated into a polar environment. (b) Fluorescence spectra of 2.5 μM **pODN** (gray line) and **pODN/RNA**($\mathbf{A_{30}}$) (black line) (50 mM sodium phosphate buffer, 0.1 M sodium chloride, pH 7.0, 25 °C). Excitation wavelength was 350 nm.

mophore is located at a hydrophobic environment of the duplex.[6] The GGG sequences in the proximity of ^{Py}**U** could contribute to the higher stability of the hairpin structure. Addition of poly(A) RNA into a **pODN** solution resulted in the opening of the hairpin structure and hybridization with poly(A) RNA because of higher thermal stability (ΔT_m = +10.2 °C). This conformation change is expected to alter the micropolarity around the pyrenecarboxamide chromophore of ^{Py}**U** and recover the fluorescence emission. Fluorescence measurements of 2.5 μM **pODN** or a DNA–RNA duplex **pODN/RNA(A$_{30}$)** were performed in sodium phosphate buffer (pH 7.0) and 100 mM sodium chloride (Fig. 3b). The fluorescence of a hairpin pODN was almost quenched (Φ_F = 0.038). In contrast, the fluorescence spectra of **pODN/RNA(A$_{30}$)** showed strong fluorescence emission at 440 nm (Φ_F = 0.51). The fluorescence intensity obtained from **pODN/RNA(A$_{30}$)** was 14 times larger than that from **pODN**. In addition, to examine the influence of the presence of nonspecific RNAs, the fluorescence intensity at the 440 nm peak obtained from the solution containing 2.5 μM **pODN/RNA(A$_{30}$)** duplex (10 μg) was evaluated before and after adding 120 μg of total RNA extracted from HeLa cells. No significant change in the fluorescence spectrum was observed, indicating that nonspecific interaction of the pyrenecarboxamide chromophore of ^{Py}**U** was negligible (Fig. 4).

To examine the effect of the probe binding length on poly(A) RNA, the changes in the thermal stability and fluorescence intensity of the duplexes formed between **pODN** and RNAs with different poly(A) lengths, **RNA(A$_n$)** (n = 21, 24, 27, and 30), were evaluated (Fig. 5). The T_m values of **pODN/RNA(A$_n$)** (2.5 μM) measured in 50 mM sodium phosphate (pH 7.0) and 100 mM sodium chloride decreased with the decreasing number of A of RNA. In particular the T_m value dropped off rapidly below n = 24. This large decrease indicates that the number of base pairs between **pODN** and **RNA(A$_n$)** decreases when n is below 24 and thus **pODN** recognizes approximately 24 bases of poly(A) RNA. The fluorescence intensity of **pODN/RNA(A$_n$)** also exhibited almost the same behavior depending on

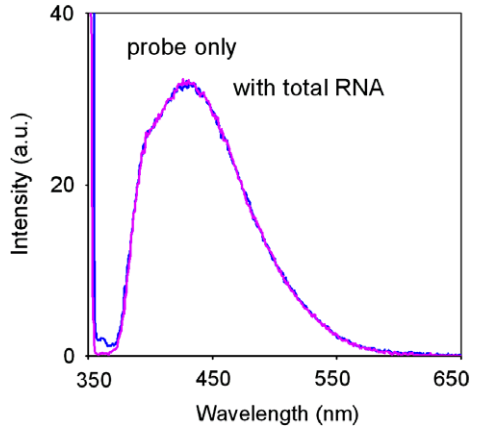

Figure 4. Fluorescence spectra of 2.5 μM **pODN/RNA(A$_{30}$)** in the presence (blue line) or absence (magenta line) of 120 μg of total RNA extracted from HeLa cell (50 mM sodium phosphate buffer, 0.1 M sodium chloride, pH 7.0, 25 °C). Excitation wavelength was 350 nm.

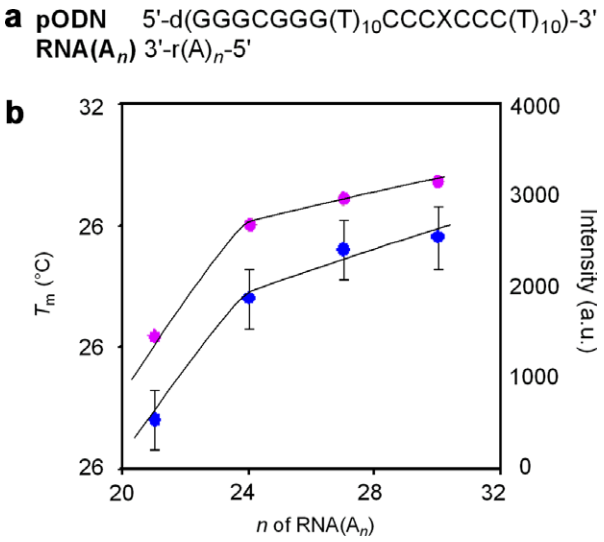

Figure 5. Length of poly(A) RNA recognized by **pODN**. (a) Sequence of **pODN/RNA(A$_n$)** (n = 21, 24, 27, and 30). (b) The influence of the length of poly(A) RNA on the thermal stability and fluorescence emission of duplexes formed with **pODN**. The T_m values were measured using 2.5 μM **pODN/RNA(A$_n$)** (50 mM sodium phosphate buffer, 0.1 M sodium chloride, pH 7.0) (blue plots). The temperature was raised by 1 °C/min from 5 °C to 90 °C, and the absorption change was monitored at 260 nm. Fluorescence intensities of 2.5 μM **pODN/RNA(A$_n$)** at 25 °C (magenta plots). Excitation wavelength was 350 nm.

the number of A in the hybridizing **RNA(A$_n$)**. These results suggest that the formation of a stable higher-ordered structure by hybridization between **pODN** and poly(A) RNA plays a critical role in the higher fluorescence emission of **pODN**.

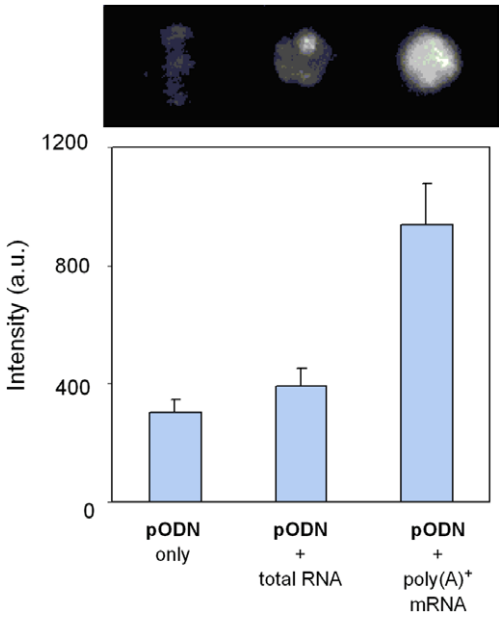

Figure 6. Fluorescence image of the samples containing 2.5 μM **pODN** and 2 μg of total RNA or poly(A)$^+$ mRNA extracted from HeLa cells (50 mM sodium phosphate, 0.1 M sodium chloride, pH 7.0, 25 °C). Fluorescence was observed using a fluorescence imager equipped with a 290–365 nm transilluminator. The image was taken through a 380 nm long pass emission filter. The data points represent the average of three experimental runs and the 15% error bars are retained from the individual data sets.

Having established poly(A)-selective fluorescence emission by **pODN**, we performed fluorescence labeling of poly(A) tracts in mRNA (Fig. 6). The fluorescence of **pODN** (2.5 μM) was evaluated after **pODN** was added to a solution containing 2 μg of total RNA or 2 μg of poly(A)$^+$ mRNA, which was prepared from total RNA with oligo-dT beads. The fluorescence was observed immediately without any washing process. In the presence of total RNA, the solution showed a slightly stronger fluorescence compared with that of **pODN** alone. On the other hand, strong fluorescence emission was obtained from the sample with concentrated poly(A)$^+$ RNA. **pODN** worked as an effective label for poly(A) tracts in mRNA.

3. Conclusion

In conclusion, we have designed a ^{Py}**U**-containing fluorescence probe for the labeling of RNA poly(A) tracts. The change in micropolarity around a pyrenecarboxamide chromophore caused by hybridization with the target RNA regulated the fluorescence emission of ^{Py}**U**. Fluorescence measurement using this probe does not require any fluorescence quencher or washing process to suppress the fluorescence emission from nonbinding probes and nonspecific binding probes. This function would be advantageous for detection of mRNAs with poly(A) tracts in cells. Therefore, this probe is a conceptually new design for efficient RNA detection.

4. Experimental

4.1. General information

^{1}H NMR spectra were measured with Varian Mercury 400 (400 MHz) spectrometer. ^{13}C NMR spectra were measured with JEOL JNM α-500 (125 MHz) spectrometer. Coupling constants (*J* value) are reported in hertz. The chemical shifts are expressed in ppm downfield from tetramethylsilane, using residual chloroform (δ = 7.24 in ^{1}H NMR, δ = 77.0 in ^{13}C NMR) as an internal standard. FAB mass spectra were recorded on JEOL JMS DX-300 spectrometer or JEOL JMS SX-102A spectrometer. Masses of ODNs were determined with a MALDI-TOF mass spectroscopy (acceleration voltage 21 kV, negative mode) with 2′,3′,4′-trihydroxyacetophenone (THAP) as matrix, using T_8 ([M−H]$^-$ 2370.61) and T_{17} ([M−H]$^-$ 5108.37) as an internal standard. HPLC was performed on a cosmosil 5C-18AR or CHEMCOBOND 5-ODS-H column (4.6× 150 mm) with a Gilson Chromatography Model 305 using a UV detector Model 118 at 254 nm.

4.1.1. Synthesis of ^{Py}U phosphoramidite unit. The synthesis of ^{Py}**U** phosphoramidite unit was executed according to Ref. 6a.

4.2. Oligodeoxynucleotide (ODN) synthesis and characterization

ODNs were synthesized by the conventional phosphoramidite method by using an Applied Biosystems 392 DNA/RNA synthesizer. Synthesized ODNs were purified by reverse phase HPLC on a 5-ODS-H column (10× 150 mm, elution with a solvent mixture of 0.1 M triethylammonium acetate (TEAA), pH 7.0, linear gradient over 30 min from 5% to 20% acetonitrile at a flow rate 3.0 mL/min). An aliquot of purified ODN solution was fully digested with calf intestine alkaline phosphatase (50 U/mL), snake venom phosphodiesterase (0.15 U/mL), and P1 nuclease (50 U/mL) at 37 °C for 3 h. Digested solution was analyzed by HPLC on Cosmosil 5C-18AR or CHEMCOBOND 5-ODS-H column (4.6× 150 mm, elution with a solvent mixture of 0.1 M triethylammonium acetate (TEAA), pH 7.0, linear gradient over 20 min from 0% to 20% acetonitrile at a flow rate 1.0 mL/min). Concentration of each ODN was determined by comparing a given peak area with those of 0.1 mM standard solution containing dA, dC, dG, and dT. Each ODN was characterized by MALDI-TOF MS. **ODN**(^{Py}**U**) 5′-d(CGCAAT^{Py}**U**TAACGC)-3′: MALDI-TOF [(M−H)$^-$] calcd 4184.85, found 4185.62. **pODN**(^{Py}**U**) 5′-(GGGCGGG(T)$_{10}$CCC^{Py}**U**CCC(T)$_{10}$)-3′: ESI-TOF [(M−10H)$^{10-}$] calcd 1057.88, found 1058.81.

4.3. UV absorption measurements

ODN solutions were prepared as described in T_m measurement experiment. Absorption spectra were obtained using an Ultraspec 3000pro UV–vis spectrophotometer (Amarsham Pharmacia Biotech) at room temperature using 1 cm path length cell.

4.4. Melting temperature (T_m) measurements

All T_ms of the ODNs (2.5 μM, final duplex concentration) were taken in 50 mM sodium phosphate buffers (pH 7.0) containing 100 mM sodium chloride. Absorbance versus temperature profiles were measured at 260 nm using a Shimadzu UV-2550 spectrophotometer equipped with a Peltier temperature controller using 1 cm path length cell. The absorbance of the samples was monitored at 260 nm from 5 °C to 90 °C with a heating rate of 1 °C/min. From these profiles, first derivatives were calculated to determine T_m values.

4.5. Fluorescence experiments

ODN solutions were prepared as described in T_m measurement experiment. Fluorescence spectra were obtained using a Shimadzu RF-5300PC spectrofluorophotometer at 25 °C using 1 cm path length cell. The excitation bandwidth was 1.5 nm. The emission bandwidth was 1.5 nm. The fluorescence quantum yields (Φ_F) were determined using 9,10-diphenylanthracene as a reference with a known Φ_F of 0.95 in ethanol according to Ref. 7. The area of the emission spectrum was integrated using the software available in the instrument, and the quantum yield was calculated according to the following equation:

$$\Phi_{F(S)}/\Phi_{F(R)} = [A_{(S)}/A_{(R)}] \times [(\mathrm{Abs})_{(R)}/(\mathrm{Abs})_{(S)}] \times [n^2_{(S)}/n^2_{(R)}].$$

Here, $\Phi_{F(S)}$ and $\Phi_{F(R)}$ are the fluorescence quantum yield of the sample and the reference, respectively. $A_{(S)}$ and $A_{(R)}$ are the area under the fluorescence spectra of the sample and the reference, respectively, $(Abs)_{(S)}$ and $(Abs)_{(R)}$ are the respective optical densities of the sample and the reference solution at the wavelength of excitation, and $n_{(S)}$ and $n_{(R)}$ are the values of refractive index for the respective solvents used for the sample (1.333) and the reference (1.383).

Fluorescence imaging was performed using Bio-Rad VersaDoc 3000. The sample solution was illuminated with a 290–365 nm transilluminator. Image was taken through a 380-nm long pass emission filter.

4.6. Extraction of total RNA from HeLa cell and purification of poly(A)$^+$ mRNA

Total RNA was prepared from HeLa cells using Trizol reagent (Invitrogen) according to the manufacturer's instruction. Briefly, 10^7 cells were homogenized in 5 mL of Trizol using Polytron, and the homogenates were further incubated for 5 min at 55 °C to promote complete dissociation of nucleoprotein complexes. After adding 1 mL of chloroform, the samples were vigorously shaken for 1 min, centrifuged at 21,000*g* for 5 min, and RNA was precipitated by adding 2.5 mL of isopropanol to the aqueous phase. After centrifugation at 21,000*g* for 5 min, the RNA pellets were dissolved in TE (10 mM Tris, 1 mM EDTA, pH 8.0) at a concentration of 1 μg/μL. Poly(A)$^+$ enriched RNA was purified from the total RNA using Quick-prep micro mRNA purification kit (GE healthcare) according to the manufacturer's instruction. Typically, 100 μg of total RNA from HeLa cells yielded 10 μg poly(A)$^+$ enriched RNA.

Acknowledgment

We thank Dr. Shinichi Nakagawa (RIKEN) for technical instruction in cell growth and RNA extraction from HeLa cells.

References and notes

1. (a) Angerer, L. M.; Angerer, R. C. *Nucleic Acids Res.* **1981**, *9*, 2819; (b) Bauman, J. G. J.; Bentvelzen, P. *Cytometry* **1988**, *9*, 517; (c) Belloc, F.; Lacombe, F.; Dumain, P.; Mergny, J. L.; Lopez, F.; Bernard, P.; Reiffers, J.; Boisseau, M. R. *Cytometry* **1993**, *14*, 339; (d) Taneja, K. L.; Lifshitz, L. M.; Fay, F. S.; Singer, R. H. *J. Cell Biol.* **1992**, *119*, 1245; (e) Pellestor, F.; Paulasova, P.; Macek, M.; Hamamah, S. *J. Histochem. Cytochem.* **2005**, *53*, 395.
2. (a) Tyagi, S.; Kramer, F. R. *Nat. Biotechnol.* **1996**, *14*, 303; (b) Kehlenbach, R. H. *Nucleic Acids Res.* **2003**, *31*, e64.
3. (a) Okamoto, A.; Ichiba, T.; Saito, I. *J. Am. Chem. Soc.* **2004**, *126*, 8364; (b) Hwang, G. T.; Seo, Y. J.; Kim, B. H. *J. Am. Chem. Soc.* **2004**, *126*, 6528; (c) Fujimoto, K.; Shimizu, H.; Inouye, M. *J. Org. Chem.* **2004**, *69*, 3271; (d) Hrdlicka, P. J.; Babu, B. R.; Sorensen, M. D.; Wengel, J. *Chem. Commun.* **2004**, 1478; (e) Langenegger, S. M.; Haner, R. *Chem. Commun.* **2004**, 2792; (f) Christensen, U. B.; Pedersen, E. B. *Nucleic Acids Res.* **2002**, *30*, 4918; (g) Kostenko, E.; Dobrikov, M.; Phshnyi, D.; Petyuk, V. *Nucleic Acids Res.* **2001**, *29*, 3611; (h) Masuko, M.; Ohtani, H.; Ebatal, K.; Shimadzu, A. *Nucleic Acids Res.* **1998**, *26*, 5409; (i) Paris, P. L.; Langenhan, J. M.; Kool, E. T. *Nucleic Acids Res.* **1998**, *26*, 3789; (j) Lewis, F. D.; Zhang, Y.; Letsinger, R. L. *J. Am. Chem. Soc.* **1997**, *119*, 5451; (k) Telser, J.; Cruickshank, K. A.; Morrison, L. E.; Netzel, T. L.; Chan, C.-K. *J. Am. Chem. Soc.* **1989**, *111*, 7226.
4. Kalyanasundaram, K.; Thomas, J. K. *J. Phys. Chem.* **1977**, *81*, 2176.
5. de Silva, A. P.; Gunaratne, H. Q. N.; Gunnlaugsson, T.; Huxley, A. J. M.; McCoy, C. P.; Rademacher, J. T.; Rice, T. E. *Chem. Rev.* **1997**, *97*, 1515.
6. (a) Okamoto, A.; Kanatani, K.; Saito, I. *J. Am. Chem. Soc.* **2004**, *126*, 4820; (b) Okamoto, A.; Saito, Y.; Saito, I. *J. Photochem. Photobiol. C-Photochem. Rev.* **2005**, *6*, 108; (c) Okamoto, A.; Tainaka, K.; Ochi, Y.; Kanatani, K.; Saito, I. *Mol. BioSyst.* **2006**, *2*, 122; (d) Okamoto, A. *Bull. Chem. Soc. Jpn.* **2005**, *78*, 2083.
7. Morris, J. V.; Mahaney, M. A.; Huber, J. R. *J. Phys. Chem.* **1976**, *80*, 969–974.